Brain Imaging and Behavior
https://doi.org/10.1007/s11682-019-00164-x

ORIGINAL RESEARCH

Exploring characteristic features of attention-deficit/hyperactivity disorder: findings from multi-modal MRI and candidate genetic data

Jae Hyun Yoo[1] · Johanna Inhyang Kim[2] · Bung-Nyun Kim[3] · Bumseok Jeong[4,5]

Abstract

The current study examined whether machine learning features best distinguishing attention-deficit/hyperactivity disorder (ADHD) from typically developing children (TDC) can explain clinical phenotypes using multi-modal neuroimaging and genetic data. Cortical morphology, diffusivity scalars, resting-state functional connectivity and polygenic risk score (PS) from norepinephrine, dopamine and glutamate genes were extracted from 47 ADHD and 47 matched TDC. Using random forests, classification accuracy was measured for each uni- and multi-modal model. The optimal model was used to explain symptom severity or task performance and its robustness was validated in the independent dataset including 18 ADHD and 18 TDC. The model consisting of cortical thickness and volume features achieved the best accuracy of 85.1%. Morphological changes across insula, sensory/motor, and inferior frontal cortex were also found as key predictors. Those explained 18.0% of ADHD rating scale, while dynamic regional homogeneity within default network explained 6.4% of the omission errors in continuous performance test. Ensemble of PS to optimal model showed minor effect on accuracy. Validation analysis achieved accuracy of 69.4%. Current findings suggest that structural deformities relevant to salience detection, sensory processing, and response inhibition may be robust classifiers and symptom predictors of ADHD. Altered local functional connectivity across default network predicted attentional lapse. However, further investigation is needed to clarify roles of genetic predisposition.

Keywords Attention deficit hyperactivity disorder · Machine learning · Multimodal imaging · Genetic polymorphisms

Introduction

Attention-deficit/hyperactivity disorder (ADHD) is a common neurodevelopmental disorder that becomes symptomatic in early childhood (Greenhill et al. 2002). A clinical diagnosis of ADHD relies, in part, on subjective parental reporting of behavioral problems which fulfilled diagnostic criteria. However, many typically developing children (TDC) also exhibit age-appropriate hyperactivity and inattention, which may provide difficulty in distinguishing between normal and

Bung-Nyun Kim and Bumseok Jeong contributed equally to this work.

Electronic supplementary material The online version of this article (https://doi.org/10.1007/s11682-019-00164-x) contains supplementary material, which is available to authorized users.

✉ Bung-Nyun Kim
kbn1@snu.ac.kr

✉ Bumseok Jeong
bs.jeong@kaist.ac.kr

[1] Department of Psychiatry, Seoul St. Mary's Hospital, College of Medicine, The Catholic University of Korea, 222 Banpo-daero, Seocho-gu, Seoul 06591, Republic of Korea

[2] Department of Psychiatry, Hanyang University Medical Center, 222-1 Wangsimni-ro, Seongdong-gu, Seoul 04763, Republic of Korea

[3] Division of Child and Adolescent Psychiatry, Department of Neuropsychiatry, Seoul National University Hospital College of Medicine, 101 Daehak-no, Chongno-gu, Seoul 03080, Republic of Korea

[4] Laboratory of Computational Affective Neuroscience and Development, Graduate School of Medical Science and Engineering, Korea Advanced Institute for Science and Technology (KAIST), 291 Daehak-ro, Yuseong-gu, Daejeon 34141, Republic of Korea

[5] KI for Health Science and Technology, KAIST Institute, KAIST, 291 Daehak-ro, Yuseong-gu, Daejeon 34141, Republic of Korea

Published online: 18 July 2019

impaired neuro-psychiatric development (Farrant et al. 2006). Thus, considerable efforts have been made to find objective and reliable biomarkers for ADHD.

Recent studies using advanced neuroimaging techniques has revealed meaningful differences in both structural and functional architecture between TDC and children diagnosed with ADHD. Structural abnormalities have been consistently reported across fronto-temporo-parietal and fronto-cerebellar networks in ADHD (Carmona et al. 2005; Castellanos 2002; Shaw et al. 2006; Silk et al. 2016). A meta-analysis of structural MRI (sMRI) studies suggested significant volume reduction in the prefrontal area, total and right cerebral brain volumes, corpus callosum and right caudate nucleus in children diagnosed with ADHD compared to TDC (Valera et al. 2007). Indeed, Shaw and colleagues (Shaw et al. 2007a) showed delayed cortical thinning of fronto-temporal areas in children with ADHD compared to TDC. Similarly, alterations in white matter integrity, such as fractional anisotropy (FA) and mean diffusivity (MD), were consistently reported in major tracts that link frontal, occipital, and temporal cortices, corticospinal tracts, and commissural fibers (Chen et al. 2016; Chuang et al. 2013; Hamilton et al. 2008; Makris et al. 2008; Silk et al. 2009). These findings were corroborated by two recent meta-analyses of diffusion tensor imaging (DTI) studies for ADHD (Aoki et al. 2017; van Ewijk et al. 2012).

Resting-state functional MRI (R-fMRI) studies have shown both local and large-scale differences in the intrinsic functional network between TDC and ADHD. ADHD children showed decreased local spontaneous activity (Li et al. 2014) as well as reduced regional homogeneity (ReHo) (An et al. 2013; Cheng et al. 2012; Liu et al. 2010) in the medial and inferior prefrontal cortex. Furthermore, ADHD children had aberrant connectivity of large-scale network between default mode network (DMN) and central executive networks (CEN) (Castellanos et al. 2008; Kelly et al. 2008), as well as DMN and ventral attention network (Sripada et al. 2014). Inappropriate engagement of salience network connectivity to DMN relative to CEN was also reported in the ADHD group (Cai et al. 2015; Choi et al. 2013).

Taken together, these findings suggest that widespread structural and functional alterations are notably associated with ADHD. However, large heterogeneous methods and findings have yet to converge into a clear, overarching hypothesis that displays the core pathophysiology of ADHD. Integration of multi-modal neuroimaging data would offer important insights into the identification of key biomarkers and process of neural mechanism associated with ADHD (Uludag and Roebroeck 2014). However few such studies have been conducted for ADHD because of the complexity in fusion of high dimensional data from a limited number of subjects (Sui et al. 2012). Application of machine learning (ML) algorithms may help extract key features from a large dataset. While classification of ADHD from TDC recently achieved accuracy of 92.8% using the ML application on multi-modal neuroimaging data (Qureshi et al. 2016), ML has not been applied to explore neuroimaging features that may account for clinical symptoms of ADHD.

In addition, several studies have suggested high heritability estimates of ADHD (Lichtenstein et al. 2010; Sherman et al. 1997; Thapar et al. 2000). Candidate single nucleotide polymorphisms (SNPs) associated with ADHD were converged to certain neurotransmitter pathway such as norepinephrine, dopamine and glutamate. Studies have demonstrated that such genotypic variants played a significant role in various phenotypes across symptom severity (Dorval et al. 2007; Kahn et al. 2003), attentional performance (Kim et al. 2016; Park et al. 2013), and brain structure and function (Fernandez-Jaen et al. 2015; Gordon et al. 2015; Hong et al. 2015; Kim et al. 2010; Kim et al. 2018; Shaw et al. 2007b). Incorporating genetic data into neuroimaging features has been attempted in schizophrenia studies yielding higher accuracy in diagnostic classification than neuroimaging features only (Yang et al. 2010). This study suggest that genetic and neuroimaging data together may help us to better diagnose ADHD children, and enhance understading of neurobiological mechanisms of ADHD.

The current study aimed to explore crucial biomarkers to distinguish 47 ADHD children from 47 age and IQ-matched TDC, using ML algorithms on multi-measures, multi-modal neuroimaging data (sMRI, R-fMRI, DTI), and to determine the correlation between meaningful classifiers and symptom severity or task performance. We further examined whether fusion of the candidate genetic profile into optimal neuroimaging model would increase the classification accuracy. Finally, a validation analysis for 18 ADHD and 18 matched TDC subjects was conducted to test generalizability of our classification model.

Materials and methods

Participants

Participants were recruited from the study called the "ADHD translational research center: a study for the identification of the comprehensive pathophysiology of ADHD based on core neurocognitive deficits and development of biological markers of treatment response" (http://clinicaltrials.gov/show/NCT02623114). This study included a total of 191 ADHD patients and 78 typically developing children (TDC) aged 6–17 years at the Child and Adolescent psychiatry clinic in Seoul National University Hospital.

All participants were diagnosed according to the Diagnostic and Statistical Manual of Mental disorder, 4th Edition (DSM-IV) (APA 2000) criteria by board certified child and adolescent psychiatrists. A diagnosis of ADHD

was confirmed with the Korean Kiddie Schedule for Affective Disorders and Schizophrenia – Present and Lifetime version (K-SADS-PL) (Kaufman et al. 1997; Kim et al. 2004). Exclusion criteria for the ADHD group were as follows: (1) an IQ < 70, (2) any hereditary genetic disorders, (3) a current/past history of brain trauma, organic brain disorders, seizure or any neurological disorders, (4) autism spectrum disorder, communication disorder or learning disorder, (5) schizophrenia or any other childhood onset psychotic disorder, (6) major depressive disorder or bipolar disorder, (7) Tourette's syndrome or chronic motor/vocal tic disorder, (8) obsessive compulsive disorder, and (9) a history of methylphenidate treatment for >1 year or having taken methylphenidate in the previous 4 weeks. The same exclusion criteria were applied to the TDC group, with another criterion that individuals must be free of psychiatric diagnoses, including a diagnosis of ADHD. IQ was measured using the Korean Wechsler Intelligence Scale for Children Fourth Edition (K-WISC-IV) (Kwak et al. 2011).

Prior to imaging data analyses, visual inspection was performed to remove data with considerable artifacts in all T1-weighted images, DTI data, and R-fMRI data by one of authors (JHY). T1-weighted (T1w) images of each participant were thoroughly examined for quality control (QC). First, one of authors (JHY) performed visual inspection for image blurriness, head motion, distortion and abnormal structural lesions. We excluded the participants if they have any minor distortion of T1w-images or abnormal structural lesions including cyst, benign tumor or aneurysm. Blurriness and head motions of images were rated as 2 classes; 1 = Acceptable (none to minimal movement), and 2 = Unsatisfactory (mild to severe movement). Before proceed to further analysis, a study coordinator (B J) finally reviewed images rated as "Acceptable" as a part of QC.

Through our visual inspection, 117 ADHD and 51 TDC participants who had defective data in any of three imaging modalities, or missing genetic information (in training datasets) were excluded. Of remaining participants, 27 ADHD and 8 TDC participants were further excluded when we optimally matched each participant (Rosenbaum and Rubin 1983) using propensity scores on age and IQ.

Our final sample consisted of 47 ADHD and 47 TDC participants with matched demographic features. For the validation analysis, 18 ADHD and 18 TDC subjects were selected from independent neuroimaging data called "A cohort study for neurodevelopmental disorder" using the same propensity score matching procedure.

Detailed information regarding the study was provided to all participants and parents, and written informed consent was obtained prior to enrollment. The study protocol was approved by the institutional review board of Seoul National University Hospital (No. 1206–054-414).

Clinical measures

Psychiatrists affiliated with the Child and Adolescent psychiatry clinic in Seoul National University Hospital evaluated symptoms of ADHD using the Korean version of ADHD Rating Scale (K-ARS) (So et al. 2002). Participants were rated on selective attention, sustained attention, vigilance and distractibility using the Korean version of the ADHD diagnostic system, a computerized continuous performance test (CPT) (Shin et al. 2000). Two different types of stimuli, visual and an auditory cues, were used to measure attentional performance for each subject. The child's attentional performance was presented by 4 broadband variables: (1) omission errors (OE, failure to respond, a measurement of inattention), (2) commission errors (CE, false response, a measurement of impulsivity), (3) response time (RT, the average response time of the correct responses), (4) response time variability (RTV, the standard deviation of the response times of correct responses). All variables were presented in T-scores adjusted for age, with lower T-scores indicating better performance.

Image acquisition

The high resolution T1-weighted structural images, DTI and R-fMRI scans were acquired using a Siemens Trio 3 T MRI scanner (Siemens Medical Systems, Erlangen, Germany) located at Seoul National University Hospital. Safety of MRI scanning was checked prior to the scan by each subject and their parents using a checklist. During the scan, the head of each subject was stabilized with cushions and the entire scanning process was monitored by the one of the authors and a parent.

Genotyping and polygenic risk score estimation

Based on previous research, candidate single nucleotide polymorphism (SNP) in three major neurotransmission pathways was chosen for genotyping and further analyses: SNPs relevant to (1) Norepinephrine receptor, transporter and catabolism (rs1800544 and rs553668 in *ADRA2A* (Comings et al. 1999, de Cerqueira et al. 2011), rs28386840 in *SLC6A2* (Sengupta et al. 2012), and rs4680 in *COMT* (Eisenberg et al. 1999), (2) dopamine receptor and transporter (2-repeat VNTR in *DRD4* exon III region (Leung et al. 2005) and 10-repeat VNTR in *DAT1* (Cook et al. 1995), (3) glutamatergic signaling pathway (rs8049651 polymorphism in *GRIN2A* (Turic et al. 2004), rs2284411 polymorphism in *GRIN2B* (Dorval et al. 2007), rs3792452 polymorphism in *GRM7* (Mick et al. 2008), rs2269272 polymorphism in *SLC1A3* (Turic et al. 2005), and rs6265 polymorphism in *BDNF* (Kent et al. 2005)).

To estimate cumulative influence of genotypic variances, polygenic risk score (PS) was calculated using the Euclidean

distance from identified risk alleles of each norepinephrine, dopamine, glutamate and all gene cluster. Distance measures could represent the summarized influence of cluster of genes, and stand for separability, divergence, or discrimination between distinct groups (Yang et al. 2010).

Overview of neuroimaging data analysis and feature extraction

Our major hypothesis was that a model with multimodal neuroimaging datasets may lead to better classification accuracy than using single type feature subset. Furthermore, we expected that the optimal model including both PS of candidate genes and neuroimaging would increase the classification accuracy. Finally, we examined the explanatory power of the optimal classification model on clinical symptoms and behavioral phenotypes.

To examine these hypotheses, we constructed input datasets consisting of each neuroimaging modality or genetic feature matrix. Optimal model construction was established using the following subsequent steps: 1) Preprocessing and extracting features from each neuroimaging modality, 2) Establishing optimal model with ML algorithm, 3) Estimating and validating performances from multiple combination sets of features, and 4) verifying the relationship with clinical variables (Fig. 1).

Preprocessing and feature extraction of neuroimaging datasets

Five morphometric features including cortical thickness (CT), CT variability (CTV), surface area (SA), mean curvature (MC), and volume from sMRI were estimated using Freesurfer imaging analysis suites 6.0 (https://surfer.nmr.mgh.harvard.edu/) with the Destrieux atlas (Destrieux et al. 2010). 16 subcortical and regional volumes were also extracted as volumetric features by the volume based stream of Freesurfer. Furthermore, 31 substructure volumes of the hippocampus and brainstem were extracted as independent structural feature subset.

Five diffusion metrics including fractional anisotropy (FA), mean diffusivity (MD), axial diffusivity (AD), radial diffusivity (RD), and mode of anisotropy (MO) were extracted from 20 major white matter tracts using the Tract-based spatial statistics module implemented in FMRIB software library (FSL) version 5.0 (https://fsl.fmrib.ox.ac.uk/fsl/fslwiki).

R-fMRI features were extracted using two distinct analysis pipelines: Large-scale functional network connectivity (FC) and dynamic regional homogeneity. Using independent component analysis, we estimated 45 large-scale FC among 10 well-matched pairs of resting-state functional networks (RSFN) which have been suggested as representative large-scale networks across population in the study of Smith and colleagues (Smith et al. 2009). To estimate local functional connectivity across time, we used dynamic regional homogeneity approach (Deng et al. 2016; Kim et al. 2018). We first calculated mean and standard deviation of ReHo across 4 time windows (30, 60, 90, 120 s, respectively) and then determined mean dynamic ReHo (ReHo) and ReHo variability (ReHoV) as r-fMRI features. To match with structural MRI features, averaged ReHo and ReHoV were extracted according to the parcellated cortical map proposed by Destrieux and colleagues (Destrieux et al. 2010).

More detailed information about preprocessing, feature extraction procedure and comparison of the head motion parameters during R-fMRI and DTI scans were described in supplementary materials.

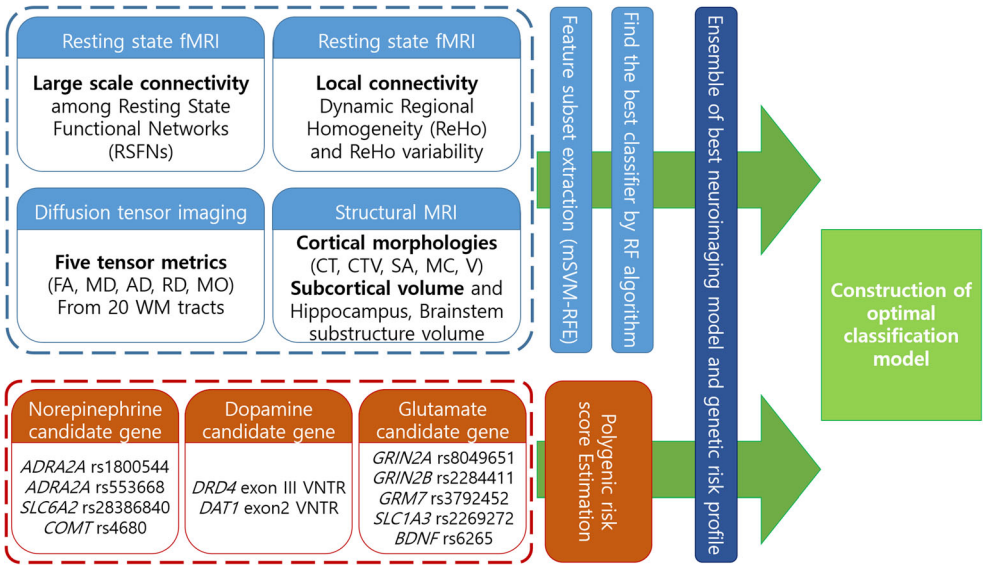

Fig. 1 Overview of feature extraction and optimal model selection algorithm. CT, Cortical thickness; CTV, Cortical thickness variability; SA, Surface area; MC, Mean curvature; V, Volume; FA, fractional anisotropy; MD, mean diffusivity; AD, axial diffusivity; RD, radial diffusivity; MO, Mode of anisotropy; mSVM-RFE multiple support vector machine recursive feature elimination; RF, randomForest

Estimation and validation of performances from multiple combination sets of features

Features extracted from multi-modal neuroimaging data had large quantity and high dimensionality (2,128 features per each participant). Such huge datasets has been associated with several disadvantages such as high computational load and over-fitting of the model (Chen and Jeong 2006). To minimize these problems, we adopted a multiple linear support vector machine - recursive feature elimination (mSVM-RFE) algorithm (Colby et al. 2012; Duan et al. 2005), which can allow us to pull out the optimal features from each uni-modal neuroimaging dataset (CT/CTV, SA/MC, volume, HC/Brainstem substructure volume, All tensors, FA/MD, AD/RD/MO, FC and ReHo/ReHoV). This algorithm dropped useless features by iterative estimation of average performance across 10-fold CV.

After selecting the best feature subsets from each modality, models were formulated and tested with two consecutive steps. First, the random Forest in the R package (https://cran.r-project.org/web/packages/randomForest/index.html) that is a decision tree based ML method was used to construct the multi-modal neuroimaging model. The random forest (RF) algorithm provides classification accuracy by using out-of-bag (OOB) error from the class labels and the importance of each feature in the model by estimating the mean squared error (Breiman 2001). Second, we performed DeLong's tests for receiver operating characteristic (ROC) curves to compare the differences of classification power between models (DeLong et al. 1988).

Optimal classification model was defined as follows: The model had the largest area under curve (AUC) and the smallest OOB error was selected as a 'Best Accuracy (BA)' model. Then, we designated another optimal classification model, 'Lesser feature with Equivalent performance' (LE), which showed the lowest OOB error with smaller number of features, while maintaining equivalent ROC characteristics compared with the BA model.

Next, ensemble of the PS score estimated from each cluster of candidate SNP data into the BA and the LE models was conducted to examine model performance. Because the BA and the LE models shared several features we illustrated the LE model as the main result. Details of the BA model findings were described in supplementary materials.

We additionally measured fitness of model using the Leave-One-Out Cross-Validation (LOOCV) algorithm in the caret package (Kuhn 2008). The Naïve-Bayes theorem was applied to estimate prediction error, which determines class by probabilities of previously seen attributes and assumes complete independence among features.

All analyses were conducted by R software packages 3.3.1. (https://cran.r-project.org/), and a significance was evaluated at a level of $p < .05$.

Relationship between important features and behavioral or cognitive symptoms

We examined the predictive power of the each BA and LE model on symptom severity and task performance using RF regression. Given the evidence that ADHD symptoms are distributed along a continuum (Stergiakouli et al. 2015), we conducted regression analyses using both ADHD and TDC datasets.

A multivariate regression model using RF has particular advantages for non-linearity assumptions, the consideration of interaction terms between predictors, and the parallel importance of the estimation of all included features (Strobl et al. 2009). Before we conducted the regression analysis, a small number of missing clinical variables were imputed (2 ADHD and 1 TDC for visual CPT, 3 ADHD and 2 TDC of auditory CPT, 9 ADHD and 4 TDC for K-ARS) using median values for each group. Then, predictive performance of both the BA or the LE model was estimated for total and subdomain scores of K-ARS and 4 broadband variables of auditory and visual CPT by RF algorithm. The importance of features included in each model was calculated as mean squared error estimates. Age, sex and IQ were also entered as predictors for RF regression.

Performance validation in the independent dataset

We tested reproducibility and robustness of each optimal subset for the classification of ADHD subject using the independent multimodal dataset. We applied the BA and the LE model to the independent dataset (18 ADHD and 18 TDC) using RF algorithm and LOOCV to replicate our results with the new participants.

Sensitivity analysis excluding high motion data

We further estimated framewise displacement (FD) of the R-fMRI to remove the high motion data suggested by Parkes and colleagues. Participants were excluded if any of the following criteria were met: (1) mFD > 0.25 mm; (2) more than 20% of the FDs were above 0.2 mm; and (3) if any FDs were greater than 5 mm. (Parkes et al. 2018).

Under a stringent regime, 9 ADHD and 3 TDC subjects in the training dataset, and 2 ADHD and 1 TDC subjects in the independent dataset were found to have high motion. Finally, 82 participants (38 ADHD and 44 TDC) in the training dataset, and 33 (16 ADHD and 17 TDC) in the independent dataset were used in the sensitivity analysis. We repeated estimation and validation of performances from each feature model in a same manner, as well as performance validation of the BA and the LE model in the independent dataset.

Results

Demographic and clinical findings

Among the training dataset, there were no significant differences in age, gender and IQ between ADHD and TDC subjects (Table 1). As expected, ADHD participants had significantly higher total K-ARS ($p < 0.001$) scores, and inattention and hyperactivity-impulsivity subdomain scores ($p < 0.001$ and $p < 0.001$, respectively) compared to TDC group. The most frequently endorsed subtypes were the predominantly inattentive type (46.8%) followed by combined type (29.8%). Attentional performance assessed by auditory CPT was significantly better in TDC compared to ADHD ($p < 0.05$ for OE, RT, and RTV), except CE score. The validation dataset showed similar demographic and clinical characteristics while relative proportion of the ADHD subtypes and auditory CPT results were different. Each of the candidate genotype variants fits the values expected based on the Hardy-Weinberg equilibrium ($p > 0.05$), except *GRIN2A* rs8049651 ($p < 0.001$). Risk allele distribution between two groups did not show any significant differences in both training and validation datasets (Table S1).

Classification performance of each unimodal neuroimaging data

The number of features comprising the optimal subsets from mSVM-RFE algorithm was various across each feature subset, ranging from 10 to 37 (Table S2). For example, ReHo/ReHoV WS20, all tensors, and CT/CTV have 36 features (e.g., ReHo of right marginal branch of the cingulate sulcus), 15 features (e.g., superior longitudinal fasciculus, MD), and 23 features (e.g., superior circular insula sulcus CT), respectively. Among R-fMRI based features, the feature subset 'ReHo/ReHoV WS20' showed the least error in 10-fold CV (28.6%) and OOB error estimates (26.6%) as well as the largest AUC in ROC analysis. Delong's test revealed superior classification performance of 'ReHo/ReHoV WS20' over 'FC' ($Z = 2.86$, $p < 0.01$) and 'ReHo/ReHoV WS30' subset ($Z = 2.00$, $p = 0.05$). Similarly, 'ReHo/ReHoV WS10' and 'ReHo/ReHoV WS40' showed comparable results to the

Table 1 Demographic and clinical characteristics of the participants

	Training dataset			Independent dataset		
	ADHD ($n = 47$)	TDC ($n = 47$)	t or χ^2	ADHD ($n = 18$)	TDC ($n = 18$)	t or χ^2
Age, y	10.06 ± 2.24	10.00 ± 2.60	0.13	9.44 ± 2.41	10.06 ± 2.69	−0.72
Male: Female, number	37:10	29:18	3.26	12:6	10:8	0.47
Full scale IQ	110.53 ± 14.38	111.19 ± 12.65	−0.24	114.17 ± 13.08	114.61 ± 14.01	−0.10
K-ARS score, total	24.18 ± 10.15	5.21 ± 5.10	10.42***	22.58 ± 8.18	5.07 ± 6.64	7.06***
Inattention	14.05 ± 5.34	3.28 ± 3.16	10.87***	12.58 ± 4.24	3.13 ± 4.42	6.55***
Hyperactivity-Impulsivity	10.13 ± 6.19	1.93 ± 2.44	7.66***	10.00 ± 5.39	1.93 ± 2.39	5.81***
ADHD subtype						
Predominantly inattentive	22 (46.8%)	–		5 (27.8%)	–	
Predominantly hyperactive-impulsive	3 (6.4%)	–		4 (22.2%)	–	
Combined	14 (29.8%)	–		5 (27.8%)	–	
Not otherwise specified	8 (17.0%)	–		4 (22.2%)	–	
Visual CPT, T-score						
OE	57.40 ± 15.70	57.52 ± 18.32	−0.34	60.18 ± 19.32	54.71 ± 17.70	−0.89
CE	63.09 ± 19.59	56.00 ± 16.58	1.87	58.18 ± 16.14	55.47 ± 13.69	−0.54
RT	53.51 ± 12.55	57.28 ± 10.68	−1.55	60.71 ± 13.42	54.94 ± 9.08	−1.51
RTV	59.47 ± 17.18	54.61 ± 16.19	1.39	58.00 ± 16.93	50.88 ± 13.78	−1.38
Auditory CPT, T-score						
OE	67.98 ± 19.51	57.84 ± 18.03	2.53*	63.47 ± 18.88	60.71 ± 19.34	−0.43
CE	62.98 ± 16.67	56.66 ± 15.44	1.85	61.71 ± 18.07	52.29 ± 11.07	−1.88
RT	57.05 ± 13.65	51.70 ± 7.54	2.27*	50.76 ± 11.53	48.82 ± 10.60	−0.53
RTV	50.07 ± 8.56	46.48 ± 8.41	1.99*	48.71 ± 10.60	46.41 ± 11.05	−0.63

ADHD, attention-deficit/hyperactivity disorder; TDC, typically developing children; K-ARS, Dupaul's ADHD rating scale, Korean version; CPT, Continuous performance test; OE, Omission error; CE, Comission error; RT, Response time; RTV, Response time variability

*$p < 0.05$, ** $p < 0.01$, *** $p < 0.001$

WS20 model, but classification performance did not differ from 'ReHo/ReHoV WS30' in the Delong's test (Z = 1.79, $p = 0.74$ and Z = 1.94, p = 0.05 respectively). 'ReHo/ReHoV WS20' was ultimately selected as the optimal feature subset for R-fMRI.

Among DTI metrics, 'All tensors' and 'AD/RD/MO' subsets equally predicted distinctions between ADHD group and TDC group, with OOB errors of 36.2%. While the 'All tensors' subset showed superior classification performance compared to the 'FA/MD' subset (Z = 2.75, p < 0.01), the comparison between 'AD/RD/MO' and 'FA/MD' did not reach the significance level (Z = 1.72, $p = 0.09$). Thus, the optimal feature subset among DTI metrics was 'All tensors'.

The 'SA/MC' subset among sMRI features showed the least errors in OOB estimates, followed by the 'CT/CTV' subset. ROC curve analysis revealed that both subsets had comparable classification performance (Z = 0.28, $p = 0.78$). The 'CT/CTV' model showed superior performance than volume (Z = 2.36, $p = 0.02$).

Performances of the multimodal models and feature-specific importance

The combination analysis of each two optimal feature subset was conducted using RF. In the double feature model, the 'CT/CTV + SA/MC' model yielded the highest AUC (0.89) and had 79.8% accuracy (Table S3). Using Delong's test, we found that the other 4 models had equivalent AUC levels to the 'CT/CTV + SA/MC' model; 'CT/CTV + Volume' (Z = 0.64, $p = 0.52$), 'All tensors + CT/CTV' (Z = 0.84, $p = 0.40$), 'All tensors + SA/MC' (Z = 0.85, $p = 0.39$), and 'ReHo/ReHoV WS20 + CT/CTV' (Z = 1.21, $p = 0.23$). Based on these results, we constructed triple, quadruple and quintuple feature models using 5 feature subsets (CT/CTV, SA/MC, Volume, All tensors, and ReHo/ReHoV WS20).

Among all combination of the neuroimaging models, 'All tensors + CT/CTV + SA/MC + Volume' was the BA model that could yield the highest AUC (0.910) and was able to predict the correct diagnosis with 83% accuracy (Fig. 2a–c). The LE model was the 'CT/CTV + Volume' model that showed the best classification performance of 85.1% (Fig. 2d, e). Features of the each neuroimaging model, along with their parametric comparison results, are shown in Table S4. The feature that displayed the highest discriminatory importance in the LE model was CT of left superior circular insula sulcus (8.8%), followed by CT of left rectus gyrus (6.5%), and CT of planum polare gyrus (6.5%).

In the LOOCV analysis, The LE model showed 23.4% misclassification error. Paired t-test revealed that error estimates of LOOCV was 4.4 ± 0.5% higher than OOB estimates across whole models (t = 6.58, $p < 0.001$).

Relationship between important features and behavioral or cognitive symptoms

The LE model explained small variance in the K-ARS total (18.0%), inattentive subdomain (18.4%), and hyperactivity-impulsivity subdomain (14.6%) scores (Fig. 3). The top 3 features explaining K-ARS total score variance were CT of left superior circular insula sulcus (12.2%), CT of the left orbital gyrus (4.4%), and CT of left posterior middle cingulate gyrus/sulcus (4.1%). Both the LE and the BA models failed to predict the 4 broadband performance scores of the CPT. However, a unimodal model with ReHo/ReHoV WS20 feature explained 6.4% of the variance of the OE in auditory CPT and predictive power was associated with ReHoV of right superior part of the precentral sulcus (7.3%), ReHo of right marginal branch of the cingulate sulcus (6.6%) and ReHoV of left medial occipito-temporal sulcus and lingual sulcus (5.3%) (Fig. 4a,b). A model 'ReHo/ReHoV WS20 + CT/CTV + SA/MC', which showed comparable ROC characteristics to the BA model, predicted the variance of the OE in auditory (4.9%) and the CE in visual CPT (5.2%), respectively (Fig. 4c, d).

Ensemble classification model using neuroimaging and candidate gene data

Classification accuracy of each genetic cluster was close to chance level (Table 2). The ensemble of each gene cluster failed to increase the classification accuracy or ROC characteristics of the LE model. The classification accuracy of the BA model was slightly increased when combining PS of the norepinephrine, dopamine or glutamate gene cluster. However, the AUC of these models did not show significant differences.

Validation of the LE and the BA models in the independent test dataset

We tested the validity of the LE and BA models on the new dataset consisting of 18 ADHD and 18 TDC participants. The LE and BA models successfully classified 69.4% (AUC = 0.65) and 77.8% (AUC = 0.70) of the independent sample, respectively (Table S5). Unfortunately, more than 30% of the independent sample lacked genetic information and clinical symptom ratings, so further analyses could not be conducted.

Results of the sensitivity analysis

Classification accuracy of each feature model was comparable to the initial results (Table S7 to S8). The BA (accuracy, 83.9%; AUC =0.89) and the LE model (accuracy, 83.9%; AUC =0.86) in the sensitivity analysis was the same as those

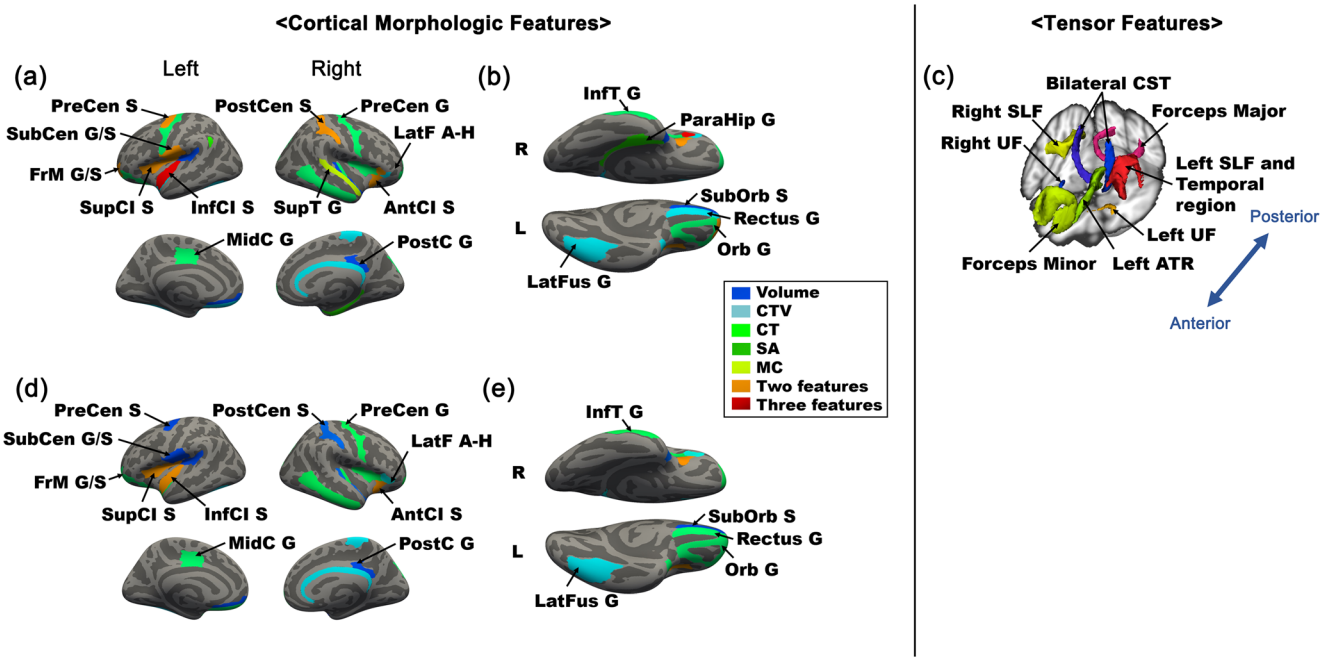

Fig. 2 Cortical morphological and Tensor features consisting optimal neuroimaging models. The schematic illustration of optimal morphological and tensor features included in the BA and the LE models. Morphological features composing the BA model were illustrated on Freesurfer surface model. (a) lateral and medial view and (b) inferior view. (c) Tensor features included in BA model were illustrated on the Johns Hopkins University White Matter Tractography Atlas. Optimal features consisting the LE model were also visualized on the (d) lateral and medial view and (e) inferior view. S, Sulcus; G, Gyrus; PreCen, Precentral; PostCen, Postcentral; SubCen, Subcentral; FrM, Frontomarginal; SupCI, Superior circular insula; InfCI, Inferior circular insula; LatF A-H, Lateral fissure, anterior ramus – horizontal; MidC, Posterior middle cingulate; PostC, Posterior dorsal cingulate; InfT, Inferior temporal; SupT, Superior temporal; SubOrb, Suborbital; Orb, Orbital; Parahip, Parahippocampal; LatFus, Lateral fusiform; CST, Corticospinal tract; SLF, Superior longitudinal fasciculus; UF, Uncinate fasciculus; ATR, Anterior thalamic radiation; ILF, Inferior longitudinal fasciculus; IFOF, Inferior fronto-occipital fasciculus; CT, Cortical thickness; CTV, Cortical thickness variability; SA, Surface area; MC, Mean curvature

of the initial classification analysis. Both the BA and the LE model in the sensitivity analysis could explain more than 18% of the K-ARS total scores, and features with high discriminatory importance were CT of left superior circular insula sulcus, and CT of right middle temporal gyrus (Table S9). Omission error of the auditory CPT could be explained by the 'ReHo WS20' (Total variance explained, 6.19%) and the 'ReHo WS20 + CT/CTV + SA/MC' (Total variance explained, 2.10%) models, and the most important feature was ReHo of the right marginal branch of the cingulate sulcus (Table S10). In the independent set, the BA model in the sensitivity analysis could correctly classified 69.7% (AUC = 0.65) of the subjects, and the LE model showed comparable results (accuracy, 69.7%; AUC = 0.61, Table S11).

Discussion

In this study, integrating features from multi-modal, multi-scale data successfully classified up to 85.1% of individuals diagnosed with ADHD from TDC. Crucial neuroimaging features for classification were CT/CTV and volume differences across widespread fronto-temporo-parietal regions. Furthermore, the interplay of features including insula, inferior frontal cortex, sensory/motor cortex, and posterior cingulate cortex explained 18.0% of the variance of the K-ARS scores. ReHo and its variability features were not included in the optimal classification model. However, regional alteration of functional connectivity modestly predicted attentional lapse and inappropriate response during CPT, while structural features could not. The ensemble of the candidate SNP data into the optimal model did not show meaningful gain in accuracy. Finally, the LE and the BA models correctly classified 69.4% and 77.8% of the diagnosis in the independent validation dataset, respectively. In sum, these results illustrated prevailing and substantial features for distinguishing ADHD from TDC and explaining relevant clinical dysfunctions.

Recently, diverse ML algorithms have been applied to unimodal neuroimaging data to achieve superior classification performance for an ADHD diagnosis, ranging in accuracy from 77 to 95% (Deshpande et al. 2015, Hart et al. 2014, Iannaccone et al. 2015, Qureshi et al. 2016, Sun et al. 2018). These promising results, however, mostly focused on comparing the classification accuracy between ML methods and included samples with disparate demographic and clinical characteristics. To date, only a handful of studies have used multimodal, multi-measure features for classification of ADHD

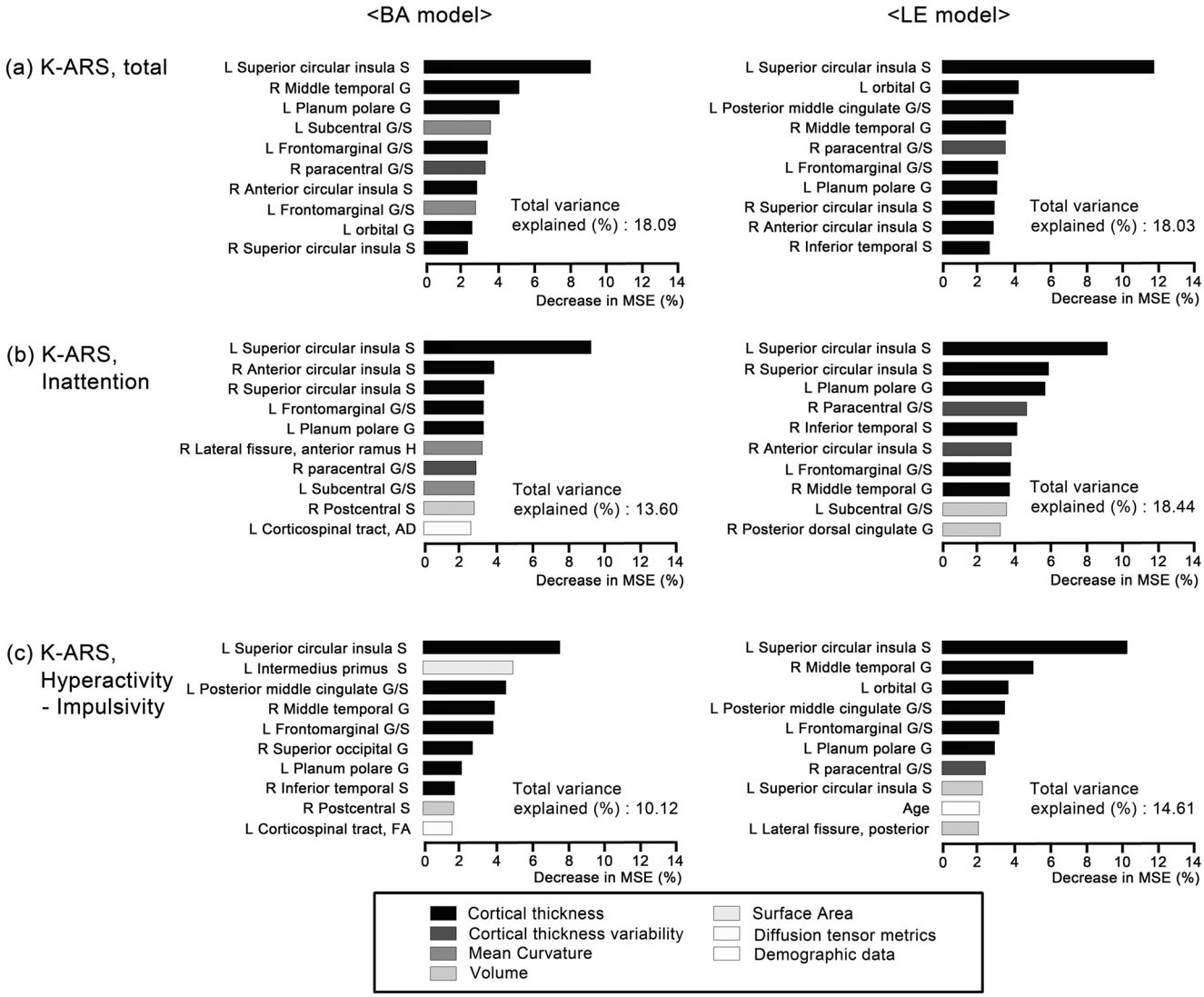

Fig. 3 Explanatory features of the BA and the LE model on the K-ARS score. (a) Total, (b) inattention, and (c) Hyperactivity-impulsivity subdomain scores of K-ARS were explained by the BA and the LE model using randomForest regression. For the visualization purpose, top 10 features of each model were depicted. The higher mean decrease MSE, the more important neuroimaging feature. K-ARS, Dupaul's ADHD scale-Korean version; BA, Best accuracy; LE, Lesser feature with equivalent performance; MSE: mean squared error; S, Sulcus; G, Gyrus; H; Horizontal; AD, Axial diffusivity; FA, Fractional anisotropy

(Colby et al. 2012, Dai et al. 2012, Qureshi et al. 2016), but the relationship between key features and clinical or behavioral symptoms have been less investigated. In this study, we demonstrated features from ML that best distinguishing between individuals with ADHD and TDC was able to predict symptom severity and task performance which could account for the brain-behavior relationships in ADHD. In addition, we combined candidate genetic data with neuroimaging feature model, which is a novel approach to ADHD classification analysis. It is important to note that our findings may have particular strengths because we included only age- and IQ-matching ADHD and TDC participants from a single neurodevelopmental clinic and collected images from a single scanner with identical parameters. Additionally, sensitivity analysis results from the low motion data chosen under a stringent regime suggest that differentiating features of ADHD, compared to TDC, is rather robust to motion artifact.

The LE model consisted of 34 morphologic features (23 CT/CTV and 11 volume) and relevant structural features were scattered across bilateral insula cortex, bilateral sensory/motor regions, and left orbitofrontal regions. In particular, reduced volume and CT of insula regions have been consistently reported in several ADHD neuroimaging studies (Lopez-Larson et al. 2012) (McLaughlin et al. 2014). It has been suggested that the insula plays a pivotal role in detecting environmentally salient stimuli and impaired function of insula is associated with attention problems such as inefficient attentional allocation (Menon and Uddin 2010). Our findings of reduced insula thickness and volume might support previous literature of aberrant salience processing in ADHD subjects (Choi et al.

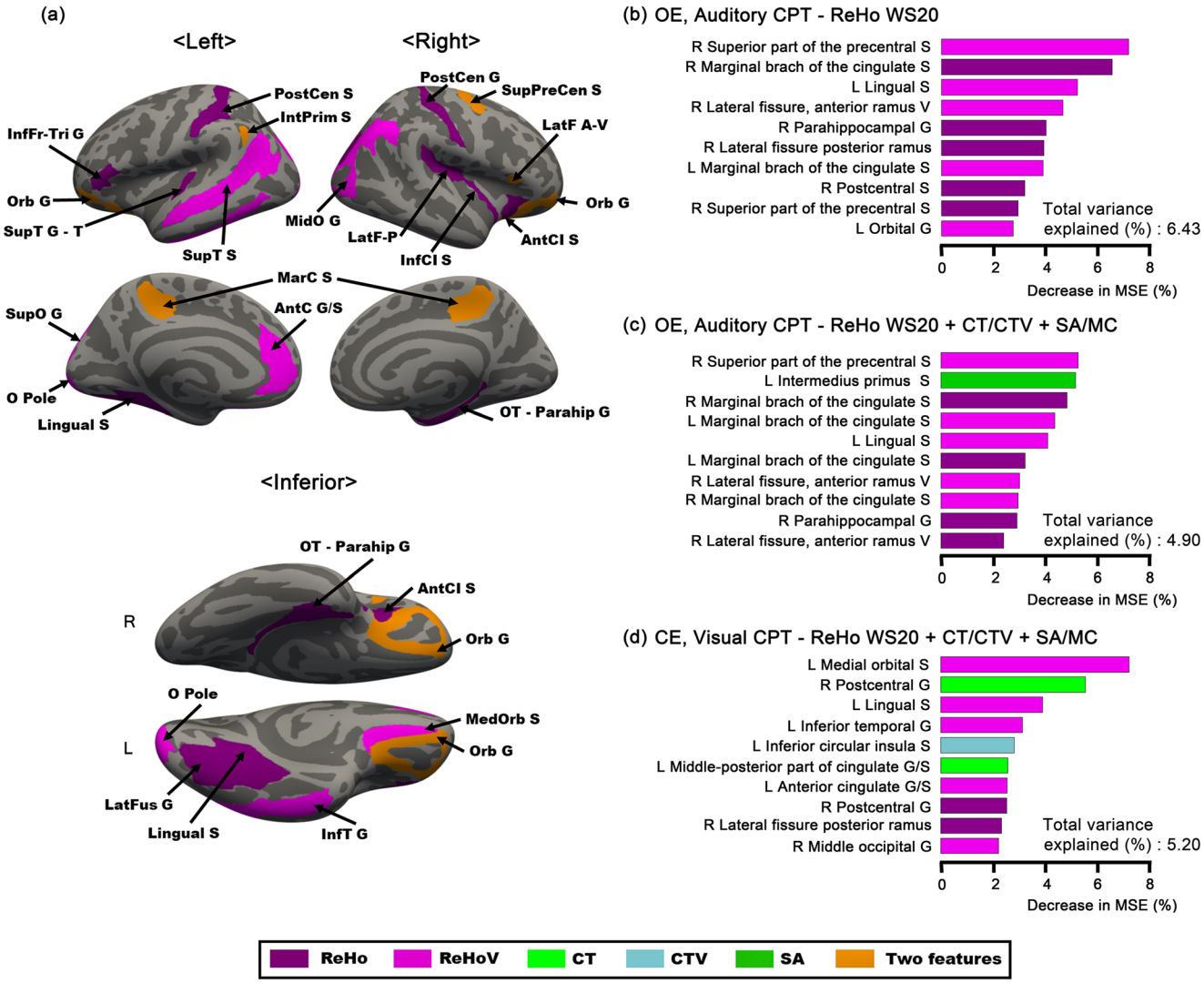

Fig. 4 Explanatory power of the models including functional feature on the CPT performance. Performances during visual and auditory CPT could be explained by the models including ReHo/ReHoV using randomForest regression. For the visualization purpose, top 10 features of each model were depicted. The higher mean decrease MSE, the more important neuroimaging feature. (a) Features included in the ReHo/ReHoV WS20 subset. Predictive power of features consisting the (b) ReHo/ReHoV WS20 model for the OE score from Auditory CPT, (c) ReHo/ReHoV WS20 + CT/CTV + SA/MC model for the OE score from Auditory CPT, and (d) ReHo/ReHoV WS20 + CT/CTV + SA/MC model for the CE score from visual CPT. CPT, Continuous performance test; ReHo, Regional homogeneity; ReHoV, Regional homogeneity variability; WS, Window size; CT, Cortical thickness; CTV, Cortical thickness variability; SA, Surface area; MC, Mean curvature; MSE, mean squared error; CE, Commission error; OE, Omission error; S, Sulcus; G, Gyrus; PreCen, Precentral; PostCen, Postcentral; SupPreCen, Superior part of the precentral; InfFr-Tri, Triangular part of the inferior frontal; Orb, Orbital; MedOrb, Medial Orbital; AntCI, Anterior circular insula; InfCI, Inferior circular insula; LatF A-V, Lateral fissure, anterior ramus – vertical; LatF-P, Lateral fissure, posterior ramus; InfT, Inferior temporal; SupT, Superior temporal; IntPrim, Intermedius primus; MidO, Middle occipital; SupO, Superior occipital; O Pole, Occipital pole, OT – Parahip, Parahippocampal part of the Occipto-Temporal, MarC, Marginal branch of the cingulate, AntC, Anterior cingulate; LatFus, Lateral fusiform

2013; Tegelbeckers et al. 2015). Clinical significance of inferior frontal region and somatosensory cortex was also reported in ADHD literature (Batty et al. 2010, Carmona et al. 2005), and these regions are known to be relevant to behavioral inhibition and sensory gating/processing (Durston et al. 2003; Vaidya et al. 2005). Taken together, morphological features include in the LE model might cover diverse aspects of ADHD pathophysiology.

More morphological (SA and MC) and multiple tensor features included in the BA model increased classification accuracy, but had negligible impact on predictive power. The BA model explained smaller amount of variance of both K-ARS subdomain scores compared to the LE model. A possible explanation for this finding is the inclusion of minor or redundant features elicited unfavorable outcomes for the regression models and had weak desirable effects in the classification analysis. This explanation is in line with the

Table 2 Classification performances of ensemble model using neuroimaging and genetic classifiers

Models	Naïve Bayes LOOCV	Metrics of RF classifier					ROC analyses AUC	Delong's test Z
		OOB error	Sensitivity	Specificity	PPV	NPV		
BA model	0.213	0.170	0.809	0.851	0.844	0.816	0.910	NA
BA model + Norepinephrine related genes	0.202	0.138	0.809	0.915	0.905	0.827	0.908	0.14
BA model + Dopamine related genes	0.213	0.128	0.830	0.915	0.907	0.843	0.912	−0.12
BA model + Glutamate related genes	0.213	0.157	0.766	0.915	0.900	0.796	0.889	1.33
BA model + All candidate genes	0.213	0.202	0.851	0.745	0.769	0.833	0.885	1.57
LE model	0.234	0.149	0.851	0.851	0.851	0.851	0.877	1.40
LE model + Norepinephrine related genes	0.234	0.160	0.851	0.830	0.833	0.848	0.861	2.01*
LE model + Dopamine related genes	0.245	0.160	0.830	0.851	0.848	0.833	0.859	1.86
LE model + Glutamate related genes	0.234	0.149	0.809	0.894	0.884	0.824	0.869	1.83
LE model + All candidate genes	0.255	0.202	0.787	0.809	0.804	0.792	0.861	2.09*
Candidate gene cluster								
Norepinephrine related genes (*ADRA2A, SLC6A2, COMT*)	0.383	0.404	0.745	0.447	0.574	0.636	0.462	5.90***
Dopamine related genes (*DAT1, DRD4*)	0.511	0.521	0.234	0.723	0.458	0.486	0.181	12.99***
Glutamate related genes (*GRIN2A, GRIN2B, GRM7, SLC1A3, BDNF*)	0.351	0.351	0.638	0.660	0.652	0.646	0.573	5.18***
All candidate genes	0.447	0.394	0.638	0.574	0.600	0.614	0.624	4.60***

Delong's Z was computed against the best accuracy model (All tensors + CT/CTV + SA/MC + Volume)

RF, randomForest; LOOCV, leave one-out cross validation; OOB error, out-of-bag error (the proportion of misclassified data); PPV, positive predictive value; NPV, negative predictive value; ROC, Receiver operating characteristic; AUC, area under curve; BA, Best accuracy; LE, Lesser feature with equivalent performance; CT, Cortical thickness; CTV, Cortical thickness variability; SA, Surface area; MC, Mean curvature

*p < 0.05, ** p < 0.01, *** p < 0.001

importance of the relevant feature selection described, especially in high-dimension feature datasets (Blum and Langley 1997).

Thus, features included in the LE model may reflect a core pathophysiology of ADHD. This assumption could be supported by the overlapping of 8 of the top 10 features between the LE and the BA models. Furthermore, morphologic alteration within bilateral insular cortices was the most importance feature for explaining the K-ARS inattentive subdomain scores while features of the posterior cingulate and temporoparietal regions were associated with the hyperactivity-impulsivity subdomain scores. These results suggest that aberrant resource allocation might be an important component of inattention and impaired social cognition and perception may be relevant to hyperactive-impulsive behaviors in ADHD.

Similar to our study, Sun and colleagues (Sun et al. 2018) examined the features relevant to ADHD based on structural MRI and DTI using RF algorithm and found that among morphological features, local alteration in cortical morphology in the left temporal lobe and left central regions was significantly relevant to ADHD. These results may underpin the hypothesis that regional changes associated with low to higher-level information processing and behavioral inhibition may play a central role in discriminating ADHD from TDC. However, there were some discrepancy between ours and Sun et al.' findings. For example, some features such as CT of bilateral cuneus, and FA of cerebral peduncle, were not significant discriminating classifiers in our study. This discrepancy may be due in part to different imaging processing and feature extraction methods as well as participant characteristics.

Functional MRI features (ReHo/ReHoV WS20) may explain the modest variance of OE of auditory CPT up to 6.4%, while the LE and the BA models were unable to predict any of task performances. Interestingly, OE of auditory CPT was a meaningful variable that exhibited brain-behavior relationship. As previous literature suggested, auditory CPT could be more useful than visual CPT for screening ADHD children who have high intelligence and mild attention problems (Shin et al. 2000). Notable differences in task performances were only found in auditory CPT (OE, RT and, RTV) in our study, as this may be resulted from age and IQ-matched ADHD and TDC participants. Decreased ReHo/ReHoV could represent a rigid connectivity state, which implies a reduced utilization of necessary resources during the attentional task (Hutchison et al. 2013). Furthermore, functional features included in the ReHo/ReHoV WS20 subset covered two hub regions of the DMN (marginal cingulate gyrus/sulcus, anterior cingulate sulcus), the salience network, the sensory/motor processing area, and the behavioral inhibition system. Altered functional connectivity of these regions have been repeatedly associated

with attentional lapse in ADHD (Derosiere et al. 2015). Our findings indicate that local connectivity features have particular advantages in predicting attentional task performance compared to structural alteration.

Fusion of candidate genetic data with optimal neuroimaging model failed to increase accuracy significantly. First, the candidate SNPs included in our study were mostly found in European descendants, and findings from East Asian are still elusive. Some putative risk alleles have been studied in Chinese population, but each association was either very weak or non-significant (Brookes et al. 2005; Qian et al. 2004; Wang et al. 2006). This genetic sequence variation between different ethnic populations could affect the PS estimation and classification performance. Second, SNPs included in current study were also associated with changes in cortical morphology (Fernandez-Jaen et al. 2015, Shaw et al. 2007b), anatomical connectivity (Chung et al. 2015) and intrinsic functional organization (Gordon et al. 2015, Kim et al. 2018, Mostert et al. 2016). Given complex interplays between polygenes and environmental exposure to psychiatric disease susceptibility (Meyer-Lindenberg and Weinberger 2006), influence of genetic variance might have been penetrated on structural and functional brain development although it has limited importance in classification. Finally, the current study only included a handful of candidate genes, so it is possible that other SNPs combined with neuroimaging features could increase classification accuracy. Therefore, further investigation may be needed to examine whether genetic data and the association with neuroimaging features predict an ADHD diagnosis.

In the independent dataset, both the LE and the BA models showed relatively high classification performance, but robustness of the BA model were superior to that of the LE model. As presented in Table S4, estimated importance of each feature in training dataset was relatively small, which could be associated with low discriminative power when applied to sample with different feature characteristics. However, RF has improved the generalization performance by ensembles of classifiers (Teng et al. 2016), and minor features consisting the BA model might play a supportive role in predicting class of the validation dataset. These minor features, such as aberrant anatomical connectivity in uncinate fasciculus, anterior thalamic radiation, forceps major and minor, corticospinal tract and superior longitudinal fasciculus, wire up fronto-temporo-parietal, fronto-limbic, and interhemispheric regions. Implication of these features to ADHD pathophysiology also have been founded in multiple studies (Aoki et al. 2017, Ben-Hur et al. 2002, van Ewijk et al. 2012). Despite such mounting evidence, more replicative evidences would be needed.

However, there are a number of limitations that should be considered. First, the findings in the present study were derived from a moderately-sized sample with the cross-sectional design. Although we could not find any prerequisites of optimal sample sizes for an imaging-genetic study with ML application, explanatory power could be limited, possibly due to a modest number of participants. Therefore, our findings should be replicated by studies with a larger sample size and a longitudinal design. Second, a small number of genetic polymorphisms were included and their functional roles have not been clearly investigated. This may hinder a straightforward interpretation of genetic influence on brain phenotype as well as clinical symptoms. Third, we adopted mSVM-RFE and RF for extraction and validation of features, but the result could be varied upon different ML algorithms. To minimize this possibility, further comparisons of classification performance and feature importance are needed.

Conclusion

The current study focused to reveal characteristic features predicting ADHD diagnosis and explaining brain-behavior relationships. Our findings suggest that ADHD children and adolescents could be best characterized by their collective structural impairment across overarching brain regions, including salient network, sensory/motor, and regions related with response inhibition. Optimal feature models could predict some of the variance of symptom severity and showed robust performance in validation dataset. Attentional lapse during tasks may be correlated with altered local functional connectivity across DMN and aforementioned regions showing structural deformity. Finally, the ensemble of candidate SNP data into the neuroimaging model may increase classification accuracy, but the effects in the current study were negligible. In sum, our finding sketched out potential utility of neuroimaging features in discriminating ADHD from TDC and explaining brain-behavior relationships associated with ADHD.

Acknowledgements This research was supported by a grant of the Brain Research Program through the National Research Foundation of Korea (NRF), funded by the Ministry of Science, ICT (NRF-2015M3C7A1028926 to B.-N.K, and NRF-2016M3C7A1914448 to B.J).

Funding This work was supported by the National Research Foundation of Korea (NRF), funded by the Ministry of Science, ICT (NRF-2015M3C7A1028926 to B.-N.K, and NRF-2016M3C7A1914448 to B.J).

Compliance with ethical standards

Conflict of interest No conflicts of interest to declare.

Ethical approval All procedures performed in studies involving human participants were in accordance with the ethical standards of the institutional and/or national research committee and with the 1964 Helsinki declaration and its later amendments or comparable ethical standards.

Informed consent Informed consent was obtained from all individual participants and their guardians included in the study.

References

An, L., Cao, Q. J., Sui, M. Q., Sun, L., Zou, Q. H., Zang, Y. F., et al. (2013). Local synchronization and amplitude of the fluctuation of spontaneous brain activity in attention-deficit/hyperactivity disorder: a resting-state fMRI study. *Neurosci Bull, 29*, (5), 603–613. https://doi.org/10.1007/s12264-013-1353-8.

Aoki, Y., Cortese, S., & Castellanos, F. X. (2017). Diffusion tensor imaging studies of attention-deficit/hyperactivity disorder: Meta-analyses and reflections on head motion. *Journal of Child Psychology and Psychiatry, 59*, 193–202. https://doi.org/10.1111/jcpp.12778.

APA. (2000). *Diagnostic and statistical manual of mental disorders : DSM-IV-TR (4th ed, text revision ed.)*. Washington, DC: American Psychiatric Association.

Batty, M. J., Liddle, E. B., Pitiot, A., Toro, R., Groom, M. J., Scerif, G., et al. (2010). Cortical gray matter in attention-deficit/hyperactivity disorder: A structural magnetic resonance imaging study. *Journal of the American Academy of Child and Adolescent Psychiatry, 49*(3), 229–238.

Ben-Hur, A., Elisseeff, A., & Guyon, I. (2002). A stability based method for discovering structure in clustered data. Pac Symp Biocomput, 6-17.

Blum, A., & Langley, P. (1997). Selection of relevant features and examples in machine learning. *Artificial Intelligence, 97*(1–2), 245–271. https://doi.org/10.1016/S0004-3702(97)00063-5.

Breiman, L. (2001). Random forests. [journal article]. *Machine Learning, 45*(1), 5–32. https://doi.org/10.1023/a:1010933404324.

Brookes, K. J., Xu, X., Chen, C. K., Huang, Y. S., Wu, Y. Y., & Asherson, P. (2005). No evidence for the association of DRD4 with ADHD in a Taiwanese population within-family study. *BMC Medical Genetics, 6*, 31. https://doi.org/10.1186/1471-2350-6-31.

Cai, W., Chen, T., Szegletes, L., Supekar, K., & Menon, V. (2015). Aberrant cross-brain network interaction in children with attention-deficit/hyperactivity disorder and its relation to attention deficits: A multisite and cross-site replication study. *Biological Psychiatry*. https://doi.org/10.1016/j.biopsych.2015.10.017.

Carmona, S., Vilarroya, O., Bielsa, A., Tremols, V., Soliva, J. C., Rovira, M., et al. (2005). Global and regional gray matter reductions in ADHD: A voxel-based morphometric study. *Neuroscience Letters, 389*(2), 88–93. https://doi.org/10.1016/j.neulet.2005.07.020.

Castellanos, F. X. (2002). Anatomic magnetic resonance imaging studies of attention-deficit/hyperactivity disorder. *Dialogues in Clinical Neuroscience, 4*(4), 444–448.

Castellanos, F. X., Margulies, D. S., Kelly, C., Uddin, L. Q., Ghaffari, M., Kirsch, A., et al. (2008). Cingulate-precuneus interactions: A new locus of dysfunction in adult attention-deficit/hyperactivity disorder. *Biological Psychiatry, 63*(3), 332–337. https://doi.org/10.1016/j.biopsych.2007.06.025.

Chen, X., & Jeong, J. C. (2006). Minimum reference set based feature selection for small sample classifications. Proc. 24th Int'l Conf. Machine learning.

Chen, L., Hu, X., Ouyang, L., He, N., Liao, Y., Liu, Q., et al. (2016). A systematic review and meta-analysis of tract-based spatial statistics studies regarding attention-deficit/hyperactivity disorder. *Neuroscience and Biobehavioral Reviews, 68*, 838–847. https://doi.org/10.1016/j.neubiorev.2016.07.022.

Cheng, W., Ji, X., Zhang, J., & Feng, J. (2012). Individual classification of ADHD patients by integrating multiscale neuroimaging markers and advanced pattern recognition techniques. *Frontiers in Systems Neuroscience, 6*, 58. https://doi.org/10.3389/fnsys.2012.00058.

Choi, J., Jeong, B., Lee, S. W., & Go, H. J. (2013). Aberrant development of functional connectivity among resting state-related functional networks in medication-naive ADHD children. *PLoS One, 8*(12), e83516. https://doi.org/10.1371/journal.pone.0083516.

Chuang, T. C., Wu, M. T., Huang, S. P., Weng, M. J., & Yang, P. (2013). Diffusion tensor imaging study of white matter fiber tracts in adolescent attention-deficit/hyperactivity disorder. *Psychiatry Research, 211*(2), 186–187. https://doi.org/10.1016/j.pscychresns.2012.11.008.

Chung, T., Ferrell, R., & Clark, D. B. (2015). Indirect association of DAT1 genotype with executive function through white matter volume in orbitofrontal cortex. *Psychiatry Research, 232*(1), 76–83. https://doi.org/10.1016/j.pscychresns.2015.01.021.

Colby, J. B., Rudie, J. D., Brown, J. A., Douglas, P. K., Cohen, M. S., & Shehzad, Z. (2012). Insights into multimodal imaging classification of ADHD. *Frontiers in Systems Neuroscience, 6*, 59. https://doi.org/10.3389/fnsys.2012.00059.

Comings, D. E., Gade-Andavolu, R., Gonzalez, N., Blake, H., Wu, S., & MacMurray, J. P. (1999). Additive effect of three noradrenergic genes (ADRA2a, ADRA2C, DBH) on attention-deficit hyperactivity disorder and learning disabilities in Tourette syndrome subjects. *Clinical Genetics, 55*(3), 160–172.

Cook, E. H., Jr., Stein, M. A., Krasowski, M. D., Cox, N. J., Olkon, D. M., Kieffer, J. E., et al. (1995). Association of attention-deficit disorder and the dopamine transporter gene. *American Journal of Human Genetics, 56*(4), 993–998.

Dai, D., Wang, J., Hua, J., & He, H. (2012). Classification of ADHD children through multimodal magnetic resonance imaging. *Frontiers in Systems Neuroscience, 6*, 63. https://doi.org/10.3389/fnsys.2012.00063.

de Cerqueira, C. C., Polina, E. R., Contini, V., Marques, F. Z., Grevet, E. H., Salgado, C. A., et al. (2011). ADRA2A polymorphisms and ADHD in adults: Possible mediating effect of personality. *Psychiatry Research, 186*(2–3), 345–350. https://doi.org/10.1016/j.psychres.2010.08.032.

DeLong, E. R., DeLong, D. M., & Clarke-Pearson, D. L. (1988). Comparing the areas under two or more correlated receiver operating characteristic curves: A nonparametric approach. *Biometrics, 44*(3), 837–845.

Deng, L., Sun, J., Cheng, L., & Tong, S. (2016). Characterizing dynamic local functional connectivity in the human brain. *Scientific Reports, 6*, 26976. https://doi.org/10.1038/srep26976.

Derosiere, G., Billot, M., Ward, E. T., & Perrey, S. (2015). Adaptations of motor neural structures' activity to lapses in attention. *Cerebral Cortex, 25*(1), 66–74. https://doi.org/10.1093/cercor/bht206.

Deshpande, G., Wang, P., Rangaprakash, D., & Wilamowski, B. (2015). Fully connected Cascade artificial neural network architecture for attention deficit hyperactivity disorder classification from functional magnetic resonance imaging data. *IEEE Trans Cybern, 45*(12), 2668–2679. https://doi.org/10.1109/TCYB.2014.2379621.

Destrieux, C., Fischl, B., Dale, A., & Halgren, E. (2010). Automatic parcellation of human cortical gyri and sulci using standard anatomical nomenclature. *Neuroimage, 53*(1), 1–15. https://doi.org/10.1016/j.neuroimage.2010.06.010.

Dorval, K. M., Wigg, K. G., Crosbie, J., Tannock, R., Kennedy, J. L., Ickowicz, A., et al. (2007). Association of the glutamate receptor subunit gene GRIN2B with attention-deficit/hyperactivity disorder. *Genes, Brain, and Behavior, 6*(5), 444–452. https://doi.org/10.1111/j.1601-183X.2006.00273.x.

Duan, K. B., Rajapakse, J. C., Wang, H., & Azuaje, F. (2005). Multiple SVM-RFE for gene selection in cancer classification with expression data. *IEEE Transactions on Nanobioscience, 4*(3), 228–234.

Durston, S., Tottenham, N. T., Thomas, K. M., Davidson, M. C., Eigsti, I. M., Yang, Y., et al. (2003). Differential patterns of striatal activation in young children with and without ADHD. *Biological Psychiatry, 53*(10), 871–878.

Eisenberg, J., Mei-Tal, G., Steinberg, A., Tartakovsky, E., Zohar, A., Gritsenko, I., et al. (1999). Haplotype relative risk study of catechol-O-methyltransferase (COMT) and attention deficit hyperactivity disorder (ADHD): Association of the high-enzyme activity Val allele with ADHD impulsive-hyperactive phenotype. *American Journal of Medical Genetics, 88*(5), 497–502.

Farrant, B. M., Fletcher, J., & Maybery, M. T. (2006). Specific language impairment, theory of mind, and visual perspective taking: Evidence for simulation theory and the developmental role of language. *Child Development, 77*(6), 1842–1853. https://doi.org/10.1111/j.1467-8624.2006.00977.x.

Fernandez-Jaen, A., Lopez-Martin, S., Albert, J., Fernandez-Mayoralas, D. M., Fernandez-Perrone, A. L., de La Pena, M. J., et al. (2015). Cortical thickness differences in the prefrontal cortex in children and adolescents with ADHD in relation to dopamine transporter (DAT1) genotype. *Psychiatry Research, 233*(3), 409–417. https://doi.org/10.1016/j.pscychresns.2015.07.005.

Gordon, E. M., Devaney, J. M., Bean, S., & Vaidya, C. J. (2015). Resting-state striato-frontal functional connectivity is sensitive to DAT1 genotype and predicts executive function. *Cerebral Cortex, 25*(2), 336–345. https://doi.org/10.1093/cercor/bht229.

Greenhill, L. L., Pliszka, S., Dulcan, M. K., Bernet, W., Arnold, V., Beitchman, J., et al. (2002). Practice parameter for the use of stimulant medications in the treatment of children, adolescents, and adults. *Journal of the American Academy of Child and Adolescent Psychiatry, 41*(2 Suppl), 26S–49S.

Hamilton, L. S., Levitt, J. G., O'Neill, J., Alger, J. R., Luders, E., Phillips, O. R., et al. (2008). Reduced white matter integrity in attention-deficit hyperactivity disorder. *Neuroreport, 19*(17), 1705–1708. https://doi.org/10.1097/WNR.0b013e3283174415.

Hart, H., Chantiluke, K., Cubillo, A. I., Smith, A. B., Simmons, A., Brammer, M. J., et al. (2014). Pattern classification of response inhibition in ADHD: Toward the development of neurobiological markers for ADHD. *Human Brain Mapping, 35*(7), 3083–3094. https://doi.org/10.1002/hbm.22386.

Hong, S. B., Zalesky, A., Park, S., Yang, Y. H., Park, M. H., Kim, B., et al. (2015). COMT genotype affects brain white matter pathways in attention-deficit/hyperactivity disorder. *Human Brain Mapping, 36*(1), 367–377. https://doi.org/10.1002/hbm.22634.

Hutchison, R. M., Womelsdorf, T., Allen, E. A., Bandettini, P. A., Calhoun, V. D., Corbetta, M., et al. (2013). Dynamic functional connectivity: Promise, issues, and interpretations. *Neuroimage, 80*, 360–378. https://doi.org/10.1016/j.neuroimage.2013.05.079.

Iannaccone, R., Hauser, T. U., Ball, J., Brandeis, D., Walitza, S., & Brem, S. (2015). Classifying adolescent attention-deficit/hyperactivity disorder (ADHD) based on functional and structural imaging. *European Child & Adolescent Psychiatry, 24*(10), 1279–1289. https://doi.org/10.1007/s00787-015-0678-4.

Kahn, R. S., Khoury, J., Nichols, W. C., & Lanphear, B. P. (2003). Role of dopamine transporter genotype and maternal prenatal smoking in childhood hyperactive-impulsive, inattentive, and oppositional behaviors. *The Journal of Pediatrics, 143*(1), 104–110. https://doi.org/10.1016/S0022-3476(03)00208-7.

Kaufman, J., Birmaher, B., Brent, D., Rao, U., Flynn, C., Moreci, P., et al. (1997). Schedule for affective disorders and schizophrenia for school-age children-present and lifetime version (K-SADS-PL): Initial reliability and validity data. *Journal of the American Academy of Child and Adolescent Psychiatry, 36*(7), 980–988. https://doi.org/10.1097/00004583-199707000-00021.

Kelly, A. M., Uddin, L. Q., Biswal, B. B., Castellanos, F. X., & Milham, M. P. (2008). Competition between functional brain networks mediates behavioral variability. *Neuroimage, 39*(1), 527–537. https://doi.org/10.1016/j.neuroimage.2007.08.008.

Kent, L., Green, E., Hawi, Z., Kirley, A., Dudbridge, F., Lowe, N., et al. (2005). Association of the paternally transmitted copy of common valine allele of the Val66Met polymorphism of the brain-derived neurotrophic factor (BDNF) gene with susceptibility to ADHD. *Molecular Psychiatry, 10*(10), 939–943. https://doi.org/10.1038/sj.mp.4001696.

Kim, Y. S., Cheon, K. A., Kim, B. N., Chang, S. A., Yoo, H. J., Kim, J. W., et al. (2004). The reliability and validity of kiddie-schedule for affective disorders and schizophrenia-present and lifetime version-Korean version (K-SADS-PL-K). *Yonsei Medical Journal, 45*(1), 81–89. https://doi.org/10.3349/ymj.2004.45.1.81.

Kim, B. N., Kim, J. W., Kang, H., Cho, S. C., Shin, M. S., Yoo, H. J., et al. (2010). Regional differences in cerebral perfusion associated with the alpha-2A-adrenergic receptor genotypes in attention deficit hyperactivity disorder. *Journal of Psychiatry & Neuroscience, 35*(5), 330–336. https://doi.org/10.1503/jpn.090168.

Kim, J. I., Kim, J. W., Park, S., Hong, S. B., Lee, D. S., Paek, S. H., et al. (2016). The GRIN2B and GRIN2A gene variants are associated with continuous performance test variables in ADHD. *Journal of Attention Disorders*, 108705471664966. https://doi.org/10.1177/1087054716649665.

Kim, J. I., Yoo, J. H., Kim, D., Jeong, B., & Kim, B. N. (2018). The effects of GRIN2B and DRD4 gene variants on local functional connectivity in attention-deficit/hyperactivity disorder. *Brain Imaging and Behavior, 12*(1), 247–257. https://doi.org/10.1007/s11682-017-9690-2 .

Kuhn, M. (2008). Caret package. *Journal of Statistical Software, 28*(5).

Kwak, G. J., Oh, S. H., & Kim, C. T. (2011). *K-WISC-IV manual for professionals*. Seoul: Hakjisa Publisher.

Leung, P. W., Lee, C. C., Hung, S. F., Ho, T. P., Tang, C. P., Kwong, S. L., et al. (2005). Dopamine receptor D4 (DRD4) gene in Han Chinese children with attention-deficit/hyperactivity disorder (ADHD): Increased prevalence of the 2-repeat allele. *American Journal of Medical Genetics. Part B, Neuropsychiatric Genetics, 133B*(1), 54–56. https://doi.org/10.1002/ajmg.b.30129.

Li, F., He, N., Li, Y., Chen, L., Huang, X., Lui, S., et al. (2014). Intrinsic brain abnormalities in attention deficit hyperactivity disorder: A resting-state functional MR imaging study. *Radiology, 272*(2), 514–523. https://doi.org/10.1148/radiol.14131622.

Lichtenstein, P., Carlstrom, E., Rastam, M., Gillberg, C., & Anckarsater, H. (2010). The genetics of autism spectrum disorders and related neuropsychiatric disorders in childhood. *The American Journal of Psychiatry, 167*(11), 1357–1363. https://doi.org/10.1176/appi.ajp.2010.10020223.

Liu, D., Yan, C., Ren, J., Yao, L., Kiviniemi, V. J., & Zang, Y. (2010). Using coherence to measure regional homogeneity of resting-state FMRI signal. *Frontiers in Systems Neuroscience, 4*, 24. https://doi.org/10.3389/fnsys.2010.00024.

Lopez-Larson, M. P., King, J. B., Terry, J., McGlade, E. C., Yurgelun-Todd, D. (2012). Reduced insular volume in attention deficit hyperactivity disorder. *Psychiatry Research: Neuroimaging, 204*(1), 32–39.

Makris, N., Buka, S. L., Biederman, J., Papadimitriou, G. M., Hodge, S. M., Valera, E. M., et al. (2008). Attention and executive systems abnormalities in adults with childhood ADHD: A DT-MRI study of connections. *Cerebral Cortex, 18*(5), 1210–1220. https://doi.org/10.1093/cercor/bhm156.

McLaughlin, K. A., Sheridan, M. A., Winter, W., Fox, N. A., Zeanah, C. H., Nelson, C. A. (2014). Widespread reductions in cortical thickness following severe early-life deprivation: A neurodevelopmental pathway to attention-deficit/hyperactivity disorder. *Biological Psychiatry, 76*(8), 629–638.

Menon, V., Uddin, L. Q. (2010). Saliency, switching, attention and control: a network model of insula function. *Brain Structure and Function, 214*(5-6), 655–667.

Meyer-Lindenberg, A., & Weinberger, D. R. (2006). Intermediate phenotypes and genetic mechanisms of psychiatric disorders. *Nature Reviews. Neuroscience, 7*(10), 818–827. https://doi.org/10.1038/nrn1993.

Mick, E., Neale, B., Middleton, F. A., McGough, J. J., & Faraone, S. V. (2008). Genome-wide association study of response to methylphenidate in 187 children with attention-deficit/hyperactivity disorder. *American Journal of Medical Genetics. Part B, Neuropsychiatric Genetics, 147B*(8), 1412–1418. https://doi.org/10.1002/ajmg.b.30865.

Mostert, J. C., Shumskaya, E., Mennes, M., Onnink, A. M., Hoogman, M., Kan, C. C., et al. (2016). Characterising resting-state functional connectivity in a large sample of adults with ADHD. *Progress in Neuro-Psychopharmacology & Biological Psychiatry, 67*, 82–91. https://doi.org/10.1016/j.pnpbp.2016.01.011.

Park, S., Jung, S. W., Kim, B. N., Cho, S. C., Shin, M. S., Kim, J. W., et al. (2013). Association between the GRM7 rs3792452 polymorphism and attention deficit hyperacitiveity disorder in a Korean sample. *Behavioral and Brain Functions, 9*, 1. https://doi.org/10.1186/1744-9081-9-1.

Parkes, L., Fulcher, B., Yucel, M., & Fornito, A. (2018). An evaluation of the efficacy, reliability, and sensitivity of motion correction strategies for resting-state functional MRI. *Neuroimage, 171*, 415–436. https://doi.org/10.1016/j.neuroimage.2017.12.073.

Qian, Q., Wang, Y., Zhou, R., Yang, L., & Faraone, S. V. (2004). Family-based and case-control association studies of DRD4 and DAT1 polymorphisms in Chinese attention deficit hyperactivity disorder patients suggest long repeats contribute to genetic risk for the disorder. *American Journal of Medical Genetics. Part B, Neuropsychiatric Genetics, 128B*(1), 84–89. https://doi.org/10.1002/ajmg.b.30079.

Qureshi, M. N., Min, B., Jo, H. J., & Lee, B. (2016). Multiclass classification for the differential diagnosis on the ADHD subtypes using recursive feature elimination and hierarchical extreme learning machine: Structural MRI study. *PLoS One, 11*(8), e0160697. https://doi.org/10.1371/journal.pone.0160697.

Rosenbaum, P. R., & Rubin, D. B. (1983). The central role of the propensity score in observational studies for causal effects. *Biometrika, 70*(1), 41–55. https://doi.org/10.1093/biomet/70.1.41.

Sengupta, S. M., Grizenko, N., Thakur, G. A., Bellingham, J., DeGuzman, R., Robinson, S., et al. (2012). Differential association between the norepinephrine transporter gene and ADHD: Role of sex and subtype. *Journal of Psychiatry & Neuroscience, 37*(2), 129–137. https://doi.org/10.1503/jpn.110073.

Shaw, P., Lerch, J., Greenstein, D., Sharp, W., Clasen, L., Evans, A., et al. (2006). Longitudinal mapping of cortical thickness and clinical outcome in children and adolescents with attention-deficit/hyperactivity disorder. *Archives of General Psychiatry, 63*(5), 540–549. https://doi.org/10.1001/archpsyc.63.5.540.

Shaw, P., Eckstrand, K., Sharp, W., Blumenthal, J., Lerch, J. P., Greenstein, D., Clasen, L., Evans, A., Giedd, J., & Rapoport, J. L. (2007a). Attention-deficit/hyperactivity disorder is characterized by a delay in cortical maturation. *Proceedings of the National Academy of Sciences of the United States of America, 104*(49), 19649–19654. https://doi.org/10.1073/pnas.0707741104.

Shaw, P., Gornick, M., Lerch, J., Addington, A., Seal, J., Greenstein, D., et al. (2007b). Polymorphisms of the dopamine D4 receptor, clinical outcome, and cortical structure in attention-deficit/hyperactivity disorder. *Archives of General Psychiatry, 64*(8), 921–931. https://doi.org/10.1001/archpsyc.64.8.921.

Sherman, D. K., Iacono, W. G., & McGue, M. K. (1997). Attention-deficit hyperactivity disorder dimensions: A twin study of inattention and impulsivity-hyperactivity. *Journal of the American Academy of Child and Adolescent Psychiatry, 36*(6), 745–753. https://doi.org/10.1097/00004583-199706000-00010.

Shin, M. S., Cho, S. C., Chun, S. Y., & Hong, K. E. (2000). A study of the development and standardization of ADHD diagnostic system. *J Kor Acad Child Adolesc Psychiatry, 11*, 91–99.

Silk, T. J., Vance, A., Rinehart, N., Bradshaw, J. L., & Cunnington, R. (2009). White-matter abnormalities in attention deficit hyperactivity disorder: A diffusion tensor imaging study. *Human Brain Mapping, 30*(9), 2757–2765. https://doi.org/10.1002/hbm.20703.

Silk, T. J., Beare, R., Malpas, C., Adamson, C., Vilgis, V., Vance, A., et al. (2016). Cortical morphometry in attention deficit/hyperactivity disorder: Contribution of thickness and surface area to volume. *Cortex, 82*, 1–10. https://doi.org/10.1016/j.cortex.2016.05.012.

Smith, S. M., Fox, P. T., Miller, K. L., Glahn, D. C., Fox, P. M., Mackay, C. E., et al. (2009). Correspondence of the brain's functional architecture during activation and rest. *Proceedings of the National Academy of Sciences of the United States of America, 106*(31), 13040–13045. https://doi.org/10.1073/pnas.0905267106.

So, Y., Noh, J., Kim, Y., Ko, S., & Koh, Y. (2002). The reliability and validity of Korean parent and teacher ADHD rating scale. *Journal of Korean Neuropsychiatric Association, 41*(2), 283–289.

Sripada, C., Kessler, D., Fang, Y., Welsh, R. C., Prem Kumar, K., & Angstadt, M. (2014). Disrupted network architecture of the resting brain in attention-deficit/hyperactivity disorder. *Human Brain Mapping, 35*(9), 4693–4705. https://doi.org/10.1002/hbm.22504.

Stergiakouli, E., Martin, J., Hamshere, M. L., Langley, K., Evans, D. M., St Pourcain, B., et al. (2015). Shared genetic influences between attention-deficit/hyperactivity disorder (ADHD) traits in children and clinical ADHD. *Journal of the American Academy of Child and Adolescent Psychiatry, 54*(4), 322–327. https://doi.org/10.1016/j.jaac.2015.01.010.

Strobl, C., Malley, J., & Tutz, G. (2009). An introduction to recursive partitioning: Rationale, application, and characteristics of classification and regression trees, bagging, and random forests. *Psychological Methods, 14*(4), 323–348. https://doi.org/10.1037/a0016973.

Sui, J., Adali, T., Yu, Q., Chen, J., & Calhoun, V. D. (2012). A review of multivariate methods for multimodal fusion of brain imaging data. *Journal of Neuroscience Methods, 204*(1), 68–81. https://doi.org/10.1016/j.jneumeth.2011.10.031.

Sun, H., Chen, Y., Huang, Q., Lui, S., Huang, X., Shi, Y., et al. (2018). Psychoradiologic utility of MR imaging for diagnosis of attention deficit hyperactivity disorder: A Radiomics analysis. *Radiology, 287*(2), 620–630. https://doi.org/10.1148/radiol.2017170226.

Tegelbeckers, J., Bunzeck, N., Duzel, E., Bonath, B., Flechtner, H.–H., Krauel, K. (2015). Altered salience processing in attention deficit hyperactivity disorder. *Human Brain Mapping, 36*(6), 2049-2060.

Teng, L., Bingbing, N., Xinyu, W., Qingwei, G., Qianmu, L., Dong, S. (2016). On random hyper-class random forest for visual classification. *Neurocomputing, 172*, 281-289.

Thapar, A., Harrington, R., Ross, K., & McGuffin, P. (2000). Does the definition of ADHD affect heritability? *Journal of the American Academy of Child and Adolescent Psychiatry, 39*(12), 1528–1536. https://doi.org/10.1097/00004583-200012000-00015.

Turic, D., Langley, K., Mills, S., Stephens, M., Lawson, D., Govan, C., et al. (2004). Follow-up of genetic linkage findings on chromosome 16p13: Evidence of association of N-methyl-D aspartate glutamate receptor 2A gene polymorphism with ADHD. *Molecular Psychiatry, 9*(2), 169–173. https://doi.org/10.1038/sj.mp.4001387.

Turic, D., Langley, K., Williams, H., Norton, N., Williams, N. M., Moskvina, V., et al. (2005). A family based study implicates solute carrier family 1-member 3 (SLC1A3) gene in attention-deficit/hyperactivity disorder. *Biological Psychiatry, 57*(11), 1461–1466. https://doi.org/10.1016/j.biopsych.2005.03.025.

Uludag, K., & Roebroeck, A. (2014). General overview on the merits of multimodal neuroimaging data fusion. *Neuroimage, 102*(Pt 1), 3–10. https://doi.org/10.1016/j.neuroimage.2014.05.018.

Vaidya, C. J., Bunge, S. A., Dudukovic, N. M., Zalecki, C. A., Elliott, G. R., & Gabrieli, J. D. (2005). Altered neural substrates of cognitive control in childhood ADHD: Evidence from functional magnetic resonance imaging. *The American Journal of Psychiatry, 162*(9), 1605–1613. https://doi.org/10.1176/appi.ajp.162.9.1605.

Valera, E. M., Faraone, S. V., Murray, K. E., & Seidman, L. J. (2007). Meta-analysis of structural imaging findings in attention-deficit/hyperactivity disorder. *Biological Psychiatry, 61*(12), 1361–1369. https://doi.org/10.1016/j.biopsych.2006.06.011.

van Ewijk, H., Heslenfeld, D. J., Zwiers, M. P., Buitelaar, J. K., & Oosterlaan, J. (2012). Diffusion tensor imaging in attention deficit/hyperactivity disorder: A systematic review and meta-analysis. *Neuroscience and Biobehavioral Reviews, 36*(4), 1093–1106. https://doi.org/10.1016/j.neubiorev.2012.01.003.

Wang, B., Wang, Y., Zhou, R., Li, J., Qian, Q., Yang, L., et al. (2006). Possible association of the alpha-2A adrenergic receptor gene (ADRA2A) with symptoms of attention-deficit/hyperactivity disorder. *American Journal of Medical Genetics. Part B, Neuropsychiatric Genetics, 141B*(2), 130–134. https://doi.org/10.1002/ajmg.b.30258.

Yang, H., Liu, J., Sui, J., Pearlson, G., & Calhoun, V. D. (2010). A hybrid machine learning method for fusing fMRI and genetic data: Combining both improves classification of schizophrenia. *Frontiers in Human Neuroscience, 4*, 192. https://doi.org/10.3389/fnhum.2010.00192.